

Research and Application Progress of High-Entropy Alloys

Zhaofeng Wang^{1,2,*} and Shuai Zhang³¹ Faculty of Electrical and Control Engineering, Liaoning Technical University, Huludao 125105, China² Intelligent Manufacturing Electronic Assembly Research Institute, Nanchang Institute of Technology, Nanchang 330044, China³ Institution of Innovation and Entrepreneurship, Liaoning Institute of Science and Engineering, Jinzhou 121013, China; zhangshuai24@126.com

* Correspondence: wangzhaofeng0412@126.com; Tel.: +86-429-5310894

Abstract: With the continuous improvement of global technological levels and the increasing demand for high-performance alloy materials in national economic construction, the traditional single principal component alloy is increasingly unable to meet people's increasing service needs. High-entropy alloys play an important role in aerospace, mechanical manufacturing, biomedicine, energy development and other engineering fields because of their unique physical, chemical and mechanical properties. Based on the concept of high-entropy alloys, the high-entropy effect, lattice distortion effect, sluggish diffusion effect and cocktail effect of high-entropy alloys are represented in this paper. The common preparation methods of high-entropy alloys are summarized according to the classification of melting-casting method, mechanical alloying method and coating method. The strength and toughness, wear resistance, corrosion resistance, high temperature resistance, fatigue resistance, radiation resistance and magnetic properties of the high-entropy alloys are discussed. The application prospect of high-entropy alloys is summarized, and the future research and development direction of high-entropy alloys are prospected on this basis.

Keywords: high-entropy alloys; preparation methods; wear resistance; corrosion resistance; application prospect



Citation: Wang, Z.; Zhang, S. Research and Application Progress of High-Entropy Alloys. *Coatings* **2023**, *13*, 1916. <https://doi.org/10.3390/coatings13111916>

Academic Editor: Michał Kulka

Received: 14 October 2023

Revised: 2 November 2023

Accepted: 7 November 2023

Published: 9 November 2023



Copyright: © 2023 by the authors. Licensee MDPI, Basel, Switzerland. This article is an open access article distributed under the terms and conditions of the Creative Commons Attribution (CC BY) license (<https://creativecommons.org/licenses/by/4.0/>).

1. Introduction

As one of the three pillars of modern civilization, materials play an irreplaceable role in the process of continuous development of society. In the course of the advancement and evolution of human history from the Stone Age to the Bronze Age and then to the Iron Age, every major social change was accompanied by the emergence of new materials. The first technological revolution is based on the development of materials such as steel and copper. The second technological revolution is based on the development of alloy steel, aluminum alloy and various non-metallic materials. The third technological revolution has realized large-scale industrialization and civil production of synthetic materials and semiconductor materials. Materials are the basis of modern technology and the core of all scientific and technological progress. The development of materials has not only changed the way of human life, but has also promoted the progress of productivity and the innovation of science and technology. Composite materials, amorphous materials and high-entropy alloys are the three hotspots in the field of materials in the past 20 years. In a socio-economically developed environment with the theme of informatization, intelligent accelerated development, energy saving and emission reduction, improving the comprehensive performance of alloys is the overall goal of new material research and development. As a new type of alloy with high hardness, high heat resistance, strong corrosion resistance, high wear resistance and fatigue resistance, high-entropy alloys are different from any existing traditional alloy. As a new alloy system, high-entropy alloys have important research value and broad application prospects. Therefore, the design, preparation and application of high-entropy alloys have become an important direction for the development of new materials [1,2].

2. Concept of High-Entropy Alloys

2.1. Proposal of High-Entropy Alloys

As early as the end of the 18th century, Franz Karl Achard carried out experimental research on multicomponent alloys of five to seven elements. The innovative work was not discovered and reported until 1963 by Professor Cyril Stanley Smith, which is the earliest recorded study on high-entropy alloys. In 1993, Professor Cantor of Cambridge University first expounded the concept of multiprincipal alloys [3]. In the subsequent research work, Cantor [4] also pointed out that the traditional alloy design concept caused the lack of research on the alloy phase diagram. Under the traditional alloy design concept, the research on the endpoint or edge region of the phase diagram has been greatly developed, while the large area in the middle of the phase diagram is poorly understood, especially the phase diagram analysis of the alloy in the presence of equal moles of several or more elements. As shown in Figure 1, there is a large degree of blank area in the phase diagram of binary and ternary alloys. Therefore, it is necessary to expand and supplement the alloy phase diagram. It is generally believed that there are two ways to achieve this goal. One is to increase the alloy element content on the basis of traditional alloy design, and the other is to use an equal atom substitution method, that is, to replace individual atoms in the component with other elements. Through the above two methods, a multicomponent alloy system with closer composition can be obtained.

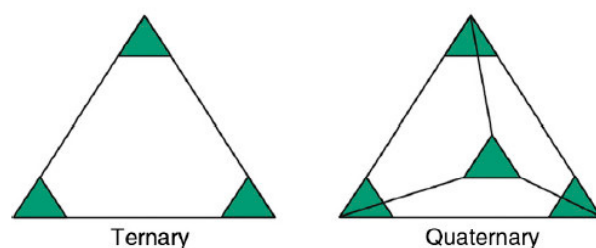


Figure 1. Schematic diagram of ternary and quaternary alloy systems [5].

Around 1995, scholars represented by Professor Yeh have also carried out a lot of basic research on multiprincipal alloy [6,7]. In 2004, Professor Yeh proposed the concept of the “high-entropy alloy” for the first time, which was expressed as: an alloy composed of five or more elements mixed in a near-equal molar ratio, with each element content (atomic ratio) greater than 5% and less than 35% [7]. On this basis, the research of multiprincipal alloys has been raised to a new height. In 2016, Lim from Singapore mentioned in an article published in Nature journal that the advent of the “high-entropy alloy” has created unprecedented broad prospects for the innovative development of materials metallurgy science, and provided new ideas and opportunities for the research and development of special property materials that can be used under extreme conditions and the upgrading and replacement of traditional materials [1].

2.2. Definition of High-Entropy Alloys

High-entropy alloys are alloys with high-entropy values. The initial definition of high-entropy alloys is based on the mixed entropy of the alloy. In physics, entropy is a physical quantity that characterizes the degree of confusion of the system. In general, the greater the number of microscopic states corresponding to a macroscopic system, the greater the entropy of the system is.

According to the principle of Boltzmann statistical thermodynamics, the entropy of a system can be expressed by the following equation:

$$S = k \ln W \quad (1)$$

In the formula, S represents the entropy of the system, k is the Boltzmann constant, $k = 1.38 \times 10^{13} \text{ J} \cdot \text{K}^{-1}$, and W is the thermodynamic probability, which represents the total

number of microscopic states in the system. Since entropy is the macroscopic property of the system and the thermodynamic probability has microscopic characteristics, this formula organically combines the macroscopic and microscopic quantities of the system and lays the foundation of statistical thermodynamics.

According to the hypothesis of Boltzmann on the relationship between entropy change and chaos degree, the mixing entropy of n principal alloy systems can be expressed as

$$\Delta S_{mix} = -R \sum x_i \ln x_i \tag{2}$$

where ΔS_{mix} is the mixing entropy, R is the molar gas constant, $8.314 \text{ J}/(\text{K}\cdot\text{mol})$, and x_i is the molar ratio of the i principal element in the alloy system. When the principal element atoms in the alloy system are equal molar ratio, the maximum mixing entropy is expressed as follows:

$$\Delta S_{mix} = R \ln n \tag{3}$$

Table 1 shows the mixing entropy of an equal molar ratio alloy system with the number of principal elements n . There is an exponential relationship between the number of principal elements and the entropy of the alloy system. With the raising of the number of principal elements in the alloy system, the mixing entropy increases continuously. The mixing entropy of the alloy system is $0.69 R$ when the two principal elements are mixed in equal molar ratio. When five kinds of principal elements are mixed to form an alloy with equal molar ratio, the mixing entropy of the alloy system is $1.61 R$.

Table 1. Mixing entropy ΔS_{mix} for the alloys with n principal elements in equal molar ratio.

n	ΔS_{mix}	n	ΔS_{mix}
1	0	11	$2.4 R$
2	$0.69 R$	12	$2.48 R$
3	$1.1 R$	13	$2.56 R$
4	$1.39 R$	14	$2.64 R$
5	$1.61 R$	15	$2.71 R$
6	$1.79 R$	16	$2.77 R$
7	$1.95 R$	17	$2.83 R$
8	$2.08 R$	18	$2.89 R$
9	$2.2 R$	19	$2.94 R$
10	$2.3 R$	20	$3 R$

Based on the deepening of the research on high-entropy alloys, Professor Yeh redefined the mixing entropy range of high-entropy alloys [6,7]. When ΔS_{mix} is less than R , it can be defined as a low-entropy alloy, when ΔS_{mix} is between $1 R$ and $1.5 R$, it can be defined as a medium-entropy alloy and for high-entropy alloys, the ΔS_{mix} is greater than $1.5 R$, as shown in Figure 2.

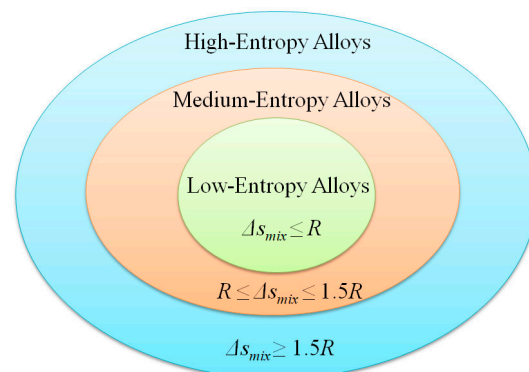


Figure 2. Schematic diagram of alloy classification.

In recent years, with the gradual deepening of the research on high-entropy alloys, the definition of high-entropy alloys has become more broad. The evaluation system also lists more alloys with good comprehensive properties as high-entropy alloys [8–14].

3. Four Effects of High-Entropy Alloys

Yeh et al. [15] firstly proposed four core effects of high-entropy alloys in 2006, namely, high-entropy effect in thermodynamics, lattice distortion effect in crystallography, sluggish diffusion effect in kinetics and cocktail effect in performance. These effects are unique in metal alloys. Most high-entropy alloys have many excellent properties which traditional alloys do not have.

3.1. High-Entropy Effect

According to the classical thermodynamic theory, the relationship between Gibbs free energy G and enthalpy H , absolute temperature T and entropy S can be expressed as follows:

$$G = H - TS \quad (4)$$

For a certain alloy system, the Gibbs free energy of the system before and after mixing changes as follows:

$$\Delta G_{mix} = \Delta H_{mix} - T\Delta S_{mix} \quad (5)$$

Here, ΔG_{mix} is the variation of Gibbs free energy and ΔH_{mix} and ΔS_{mix} represent the mixing enthalpy and mixing entropy of the alloy system, respectively. The mixing entropy and mixing enthalpy are competitive with each other. The Gibbs free energy will descend with the decrease in mixing enthalpy and the increase in mixing entropy. High-entropy alloys are more likely to form simple solid solutions due to their high mixing entropy. The schematic diagram of the formation of solid solution promoted by high-entropy effect is shown in Figure 3.

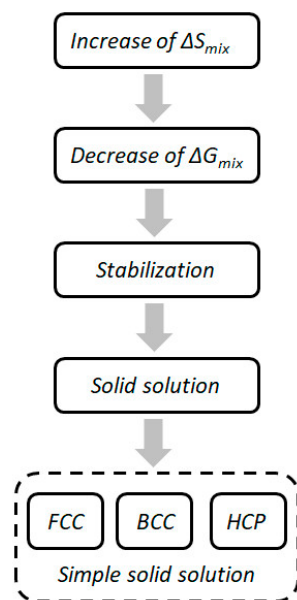


Figure 3. Schematic diagram of the formation of solid solution promoted by high-entropy effect.

The high-entropy effect of high-entropy alloys has been confirmed in many aspects [16–22]. The influence of high-entropy effect on the phase structure of high-entropy alloys is more intuitive. It can be seen from Figure 4 that the phases in quinary, senary, and septenary alloys remain rather simple. The major phases have simple structures such as BCC and FCC.

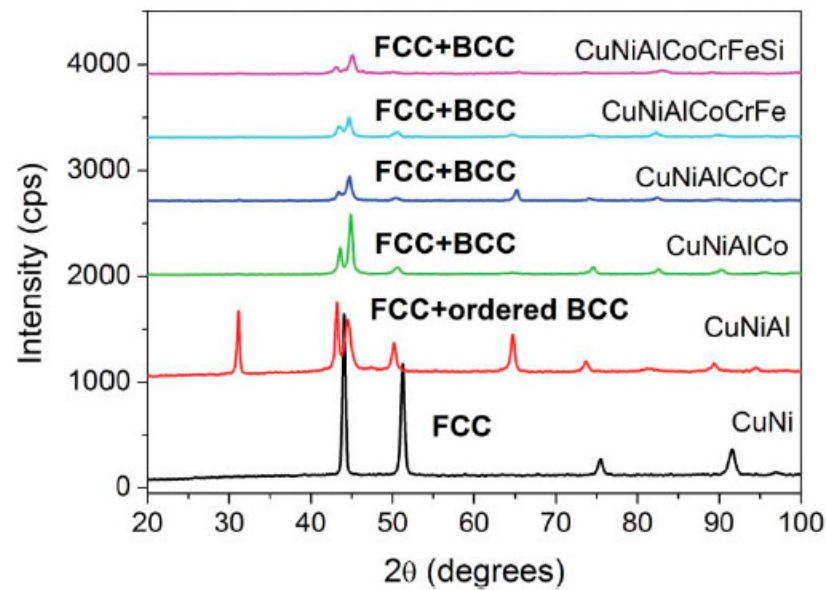


Figure 4. The effect of component increase on the XRD pattern of the alloy [23].

3.2. Lattice Distortion Effect

The high-entropy alloys can easily form a disordered solid solution because of the high-entropy effect, as shown in Figure 5. The atoms in the solid solution are randomly distributed. Each atom may be surrounded by different atoms. Each principal element will be different because of the structural characteristics. These differences will inevitably cause a certain degree of deviation in the lattice atom. Then, the lattice distortion is generated. This characteristic is called lattice distortion effect, which will have a remarkable impact on the microstructure and properties of high-entropy alloys.

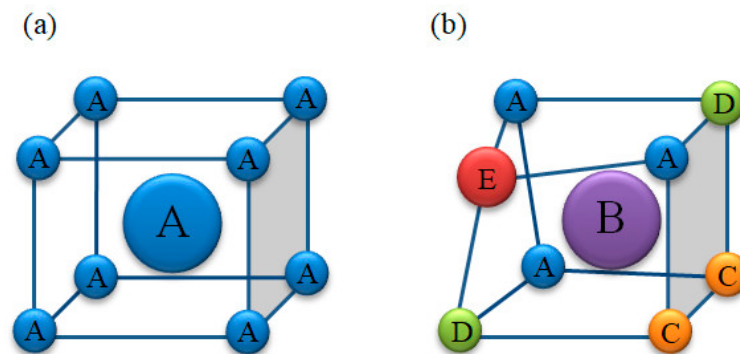


Figure 5. Schematic diagram of the lattice distortion effect. (a) BCC no lattice distortion, one component alloy; (b) BCC severe lattice distortion, five component alloy.

The lattice distortion can enlarge the X-ray scattering and reduce the diffraction peak intensity. When the atoms with different properties randomly occupy the crystal lattice position, the X-ray is scattered due to the serious distortion of each diffraction surface. Professor Yeh [24] studied the decrease in X-ray diffraction peak intensity in alloy systems in 2007. The results are shown in Figure 6. The intensity of the diffraction peak decreases with the enlargement of the number of alloying elements in high-entropy alloys. The degree of reduction is much larger than that of the thermal effect, which means that the internal lattice distortion of the alloy has an important effect on the change of X-ray diffraction peak intensity.

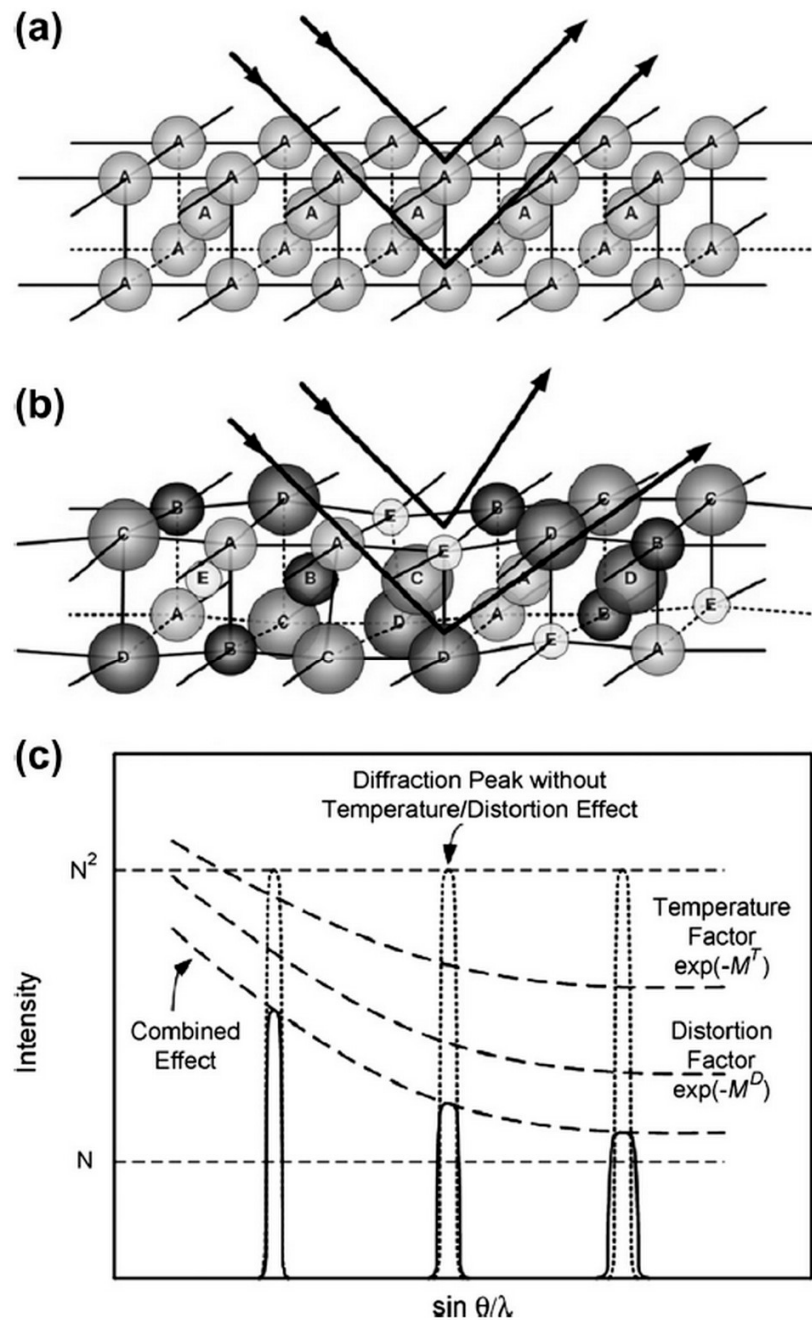


Figure 6. Schematic view of lattice distortion effect on Bragg diffraction: (a) a perfect lattice with the same atoms;(b) distorted lattices of solid solutions composed of different atoms; (c) temperature and distortion effects on the XRD intensity [24].

The serious lattice distortion will increase the scattering of electrons and phonons, which will reduce the electrical conductivity and thermal conductivity of the alloy. Research shows that the electrical conductivity and thermal conductivity of the alloy decrease with the increase in aluminum content, and are lower than pure aluminum [25]. It can be seen that the slope of the curve of the high-entropy alloys has a small positive value, while the slope of the curve of pure aluminum has a large negative value from Figure 7.

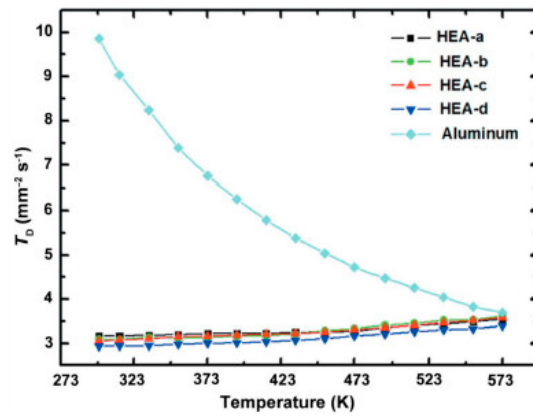


Figure 7. The curves of thermal diffusivity of pure aluminum and high-entropy alloys with temperature change [25].

3.3. Sluggish Diffusion Effect

Diffusion is the phenomenon that occurs when atoms migrate away from their original position, and the macroscopic flow of material is caused. In the process of phase transition, the formation of a new phase usually requires the cooperative diffusion of many atoms. In the liquid state, the principal elements of the high-entropy alloys are disordered due to the high-entropy effect. In the cooling process, the diffusion of the high-entropy alloys involves the diffusion and redistribution of the principal element atoms. The nucleation and growth of the new phase are inhibited. It can be called the sluggish diffusion effect in kinetics of the high-entropy alloys.

Yeh et al. [26] selected the alloy system with a single-phase face-centered cubic structure as the research object to analyze the diffusion coefficient. As shown in Figure 8, the diffusion coefficients of the five elements in high-entropy alloys are significantly smaller than those in traditional alloys.

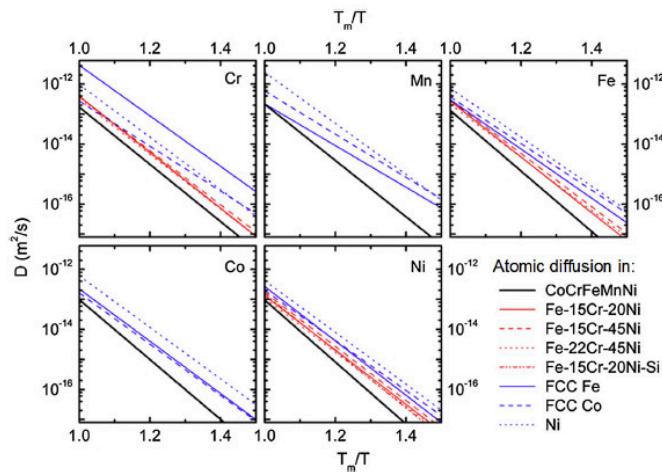


Figure 8. The relationship between the diffusion coefficient of different materials and the temperature change [26].

The sluggish diffusion effect not only promotes the formation of supersaturated solid solution and the precipitation of nanophase, but also has a beneficial effect on the comprehensive properties of high-entropy alloys [27–32]. These beneficial effects include slowing down the phase transition rate, increasing the recrystallization temperature of the alloy, inhibiting the nucleation and growth of crystal grains, improving creep properties, etc. Therefore, the sluggish diffusion effect in kinetics is beneficial to control the properties of high-entropy alloys.

3.4. Cocktail Effect

The cocktail effect was firstly proposed by Professor Ranganathan [33], as shown in Figure 9. It shows that the microstructure and properties of high-entropy alloys are determined by the various elements added, and the performance can be greatly changed by adjusting the principal component composition. Reference 7 shows that the strength of the $Al_xCoCrFeNiCu$ alloy increases with the increase in Al content, as shown in Figure 10. The phase structure of the alloy changed from FCC structure to FCC + BCC structure, and then to BCC structure. In addition, some experiments have shown that the addition of an aluminum element can reduce the density of high-entropy alloys [34]. If some refractory elements are added, the high-temperature properties can be enhanced [35]. In the alloy system, the effect of Cu contributes to the formation of an $L1_2((Ni, Cu)_3Al)$ phase [36]. It may be possible to obtain an unforeseeable high performance using the cocktail effect.

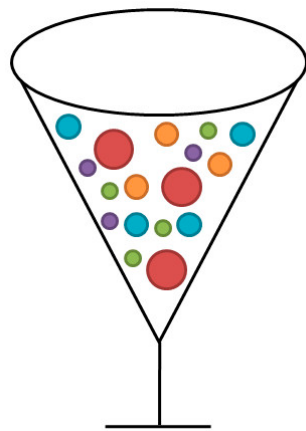


Figure 9. Schematic diagram of cocktail effect.

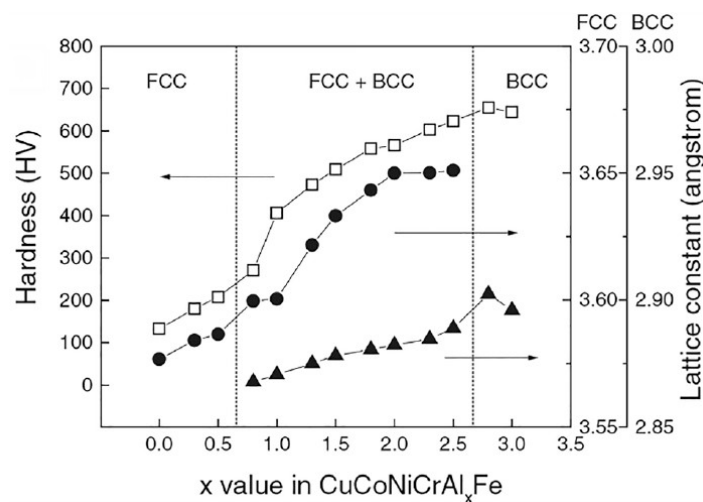


Figure 10. Comparison of hardness and lattice constant of alloy system [7].

4. Preparation Method of High-Entropy Alloys

The preparation method, production process and the selection of process parameters of high-entropy alloys have great influence on the alloy properties. Moreover, different preparation methods will lead to large differences in processing costs. Therefore, it is important to reasonably select the preparation method of high-entropy alloys and optimize the process parameters in the preparation process. After decades of production practice, it has developed from the initial vacuum arc melting-casting method [37–40] to today's mechanical alloying method [41,42], surface coating method [43–45] and other preparation methods.

4.1. Melting-Casting Method

4.1.1. Vacuum Arc Melting

The earliest preparation method of high-entropy alloys is vacuum arc melting, as shown in Figure 11. The arc discharge is used to heat and melt the metal, and then the liquid metal is cooled and solidified in this method. The high-entropy alloys firstly proposed by Yeh et al. were prepared using this method [7]. Because this method can melt metal elements with high melting points, most of the current research is also based on this method to prepare alloy ingots. However, the cooling rate of the alloy is fast during the preparation process using this method, and there will be obvious shrinkage on the metal surface during the solidification process, which is usually only suitable for the preliminary detection and analysis of the alloy.

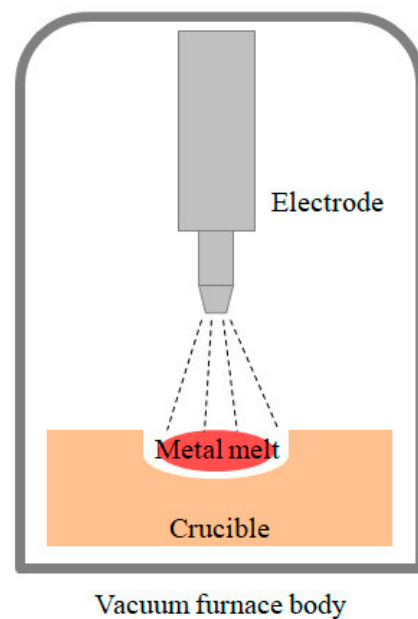


Figure 11. Schematic diagram of vacuum arc melting method.

4.1.2. Resistance Furnace Melting

Yeh et al. [6] tried to melt high-entropy alloys under atmospheric conditions. They used a resistance furnace to melt and cast CuCoNiCrCrAlFeTiV series alloys. The results show that, although the microstructure of the alloy is relatively uniform and the degree of segregation is relatively small, this method is not suitable for the melting of high-entropy alloys which are easily oxidized and have high melting points.

4.1.3. Vacuum Induction Melting

Vacuum induction melting is the process of melting metal under vacuum conditions using electromagnetic induction [46]. This method can realize the preparation of large-size ingots of high-entropy alloys, which provides enough raw materials for the further study of alloy deformation, microstructure and properties and promotes the research and application process of high-entropy alloys.

4.1.4. Vacuum Electron Beam Melting

Vacuum electron beam melting is a preparation method of high-entropy alloys. In this method, the high-energy electron beam is focused on metal raw materials in a high vacuum environment. The metal is melted and then solidified. Fujieda et al. [47] firstly applied vacuum electron beam melting technology to the preparation of high-entropy alloys in 2015. Compared with the samples melted by electric arc furnace, although the strength of the samples melted by electron beam decreased slightly, the plasticity increased by nearly

20%, and the strength limit still reached 1400 MPa. However, this method also has some limitations. There is serious anisotropic behavior exhibited in the solidification structure, and it is not suitable for the melting of volatile elements.

4.2. Mechanical Alloying Method

Mechanical alloying is the grinding of mixed powder in a high-energy ball mill and the atoms in the powder particles are diffused through repeated cold welding and fracture to achieve the alloying process. The schematic diagram of the mechanical alloying method is shown in Figure 12. Mechanical alloying is an effective method to synthesize fine crystalline powders in a non-equilibrium state. In 2008, Indian scholar Varalakshmi prepared AlCrCuFeTiZn high-entropy alloys using the mechanical alloying method for the first time [48], and the alloys showed high thermodynamic stability and good mechanical properties. Traditional manufacturing processes struggle to achieve the alloying of some special substances and the synthesis of new substances. However, the mechanical alloying technology is not limited by the physical properties of the mixing enthalpy, melting point and so on, so this difficulty can be overcome. It should be noted that the mechanical alloying method will produce some pollutants during the milling process. In addition, due to the powder state of the product prepared by mechanical alloying, the molding process of the sample needs to be completed under large pressure, the equipment condition is limited and the stamping cost is high. Therefore, the mechanical alloying method is more suitable for large-scale industrial production.

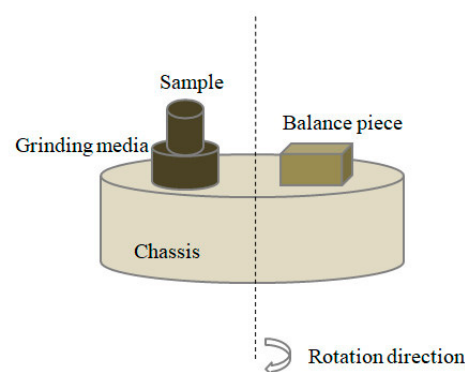


Figure 12. Schematic diagram of mechanical alloying method.

4.3. Coating Method

The coating method is an alloy preparation method that coats a coating material with excellent comprehensive performance onto the surface of an engineering component or mold to improve its service performance. High-entropy alloys are especially suitable for coating materials. At present, the common preparation methods of high-entropy alloy coatings are as follows.

4.3.1. Laser Cladding

Laser cladding is a preparation method that uses a laser beam to melt the high-entropy alloy powder and the surface of the matrix material at the same time, and forms a surface coating combined with the matrix during the subsequent solidification process, as shown in Figure 13. The molten surface has small dilution, small deformation, fast solidification speed, high stability, and reliable performance. Zhang et al. [49] prepared AlCoCrFeNi high-entropy alloy coatings by laser cladding and analyzed the effect of the Fe element on its properties. Chang et al. [50] used the laser cladding technique to prepare FeCr_xCoNiB high-entropy alloy coatings on AISI1045 steel matrix and studied its thermal stability and oxidation resistance. Huang et al. [51] prepared an equimolar ratio of TiVCrAlSi coatings using a laser cladding process and studied its wear resistance behavior. Jiang et al. [52] prepared AlCoCr_xFeNi coatings on a 45# steel matrix using laser cladding and studied its

corrosion behavior. Liu et al. [53] fabricated AlCoCrFeNiTi_x coatings on AISI1045 steel matrix by laser cladding and studied its microstructure and corrosion behavior.

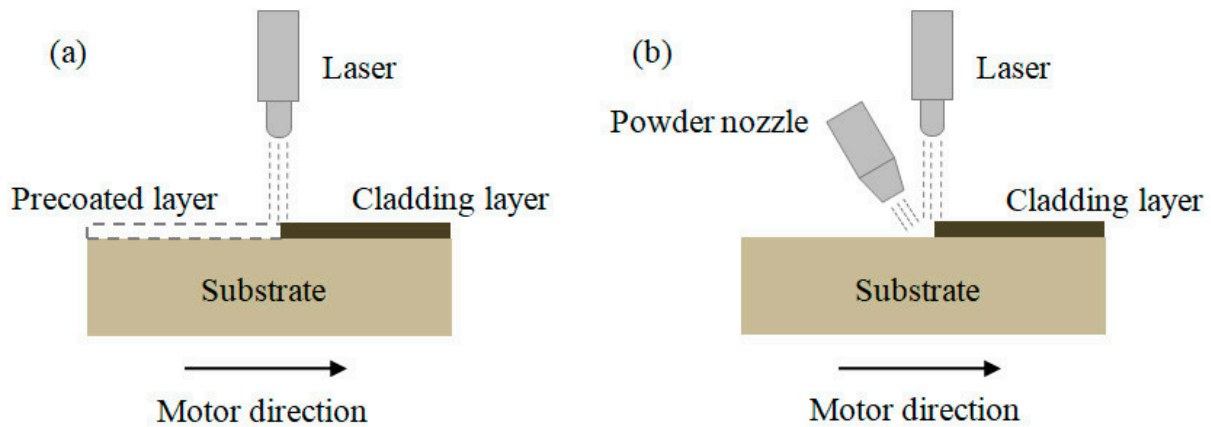


Figure 13. Schematic diagram of laser cladding method: (a) pre-coating method; (b) synchronous powder.

4.3.2. Magnetron Sputtering

Magnetron sputtering is one of the main preparation techniques for various soft and hard films. The coating uses the sputtering effect to make high-energy particles bombard the target. After the target atoms escape, they move along the established direction and deposit on the target substrate to form a film. The schematic diagram of the magnetron sputtering method is shown in Figure 14. Magnetron sputtering has been widely used in the fields of metals, semiconductors, insulators and other materials due to its advantages of low equipment cost, convenient operation, large area coating and large adhesion of the film. Chen et al. [54] prepared high-entropy alloy nitride films by magnetron sputtering with a hardness of more than 40 GPa. Chang et al. [55] found that the increasing of nitrogen flow rate will promote the crystallization of the amorphous high-entropy film of TiVCrAlZr and transform it into FCC solid solution. Lin et al. [56] found that boron can improve the hardness of FeCoCrNiAlB_x sputtering coating and change the wear mechanism. Huang et al. [57,58] researched the effect of substrate bias and temperature on the film structure. Chen et al. [59] prepared VAlTiCrMo coatings by magnetron sputtering technology. Huo et al. [60] used nanocrystalline CoCrFeNi high-entropy alloy films formed by magnetron sputtering.

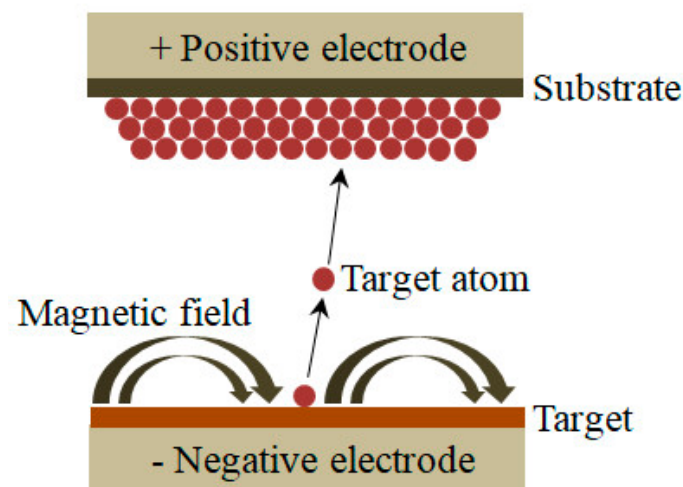


Figure 14. Schematic diagram of magnetron sputtering method.

4.3.3. Thermal Spray Technology

Thermal spraying technology is a coating technology that uses a heat source to heat the spraying material and uses high pressure gas to make the molten coating move at a high speed, and finally deposits it on the surface of the substrate to form a film, as shown in Figure 15. Thermal spray coating has little effect on the matrix, and the process is simple to operate, easy to control, low cost, easy to scale for industrial production and has great potential for industrial application. Huang et al. [61] firstly used thermal spraying technology to prepare coatings and broadened the preparation method. Since then, scholars have carried out research in this field. Ang et al. [62] used the plasma spraying method to prepare AlCoCrFeNi and MnCoCrFeNi coatings. Wang et al. [63] found that (CoCrFeNi)₉₅Nb₅ coating showed typical selective corrosion and good corrosion resistance in the corrosion resistance test. Chen et al. [64] prepared Al_{0.6}TiCrFeCoNi coating by flame spraying method, and the test showed that the coating had good wear resistance.

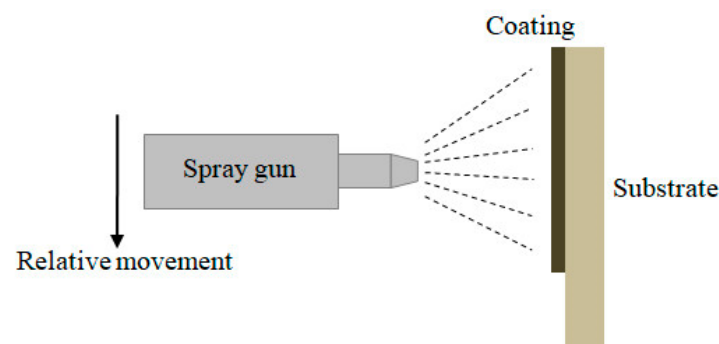


Figure 15. Schematic diagram of thermal spraying technology.

4.3.4. Electrochemical Deposition Method

Electrochemical deposition is deposited on the surface of the matrix to form a coating under the action of an electric field. The schematic diagram of the electrochemical deposition method is shown in Figure 16. It is a low-cost coating preparation method, and it is very suitable for the preparation of alloy materials with nanostructures. Moreover, the phase composition, morphology and thickness of the coating can be easily controlled. Yao et al. [65] firstly prepared high-entropy alloy films by electrochemical deposition technology and successfully prepared BiFeCoNiMn high-entropy alloy films. Soare et al. [66] prepared two coatings on copper substrates by electrochemical deposition. Aliy et al. [67] prepared AlFeCoNiCu high-entropy alloy graphene oxide coating on low carbon steel substrate by electrochemical deposition, and explored the effect of graphene oxide on the microstructure and corrosion properties of the coating.

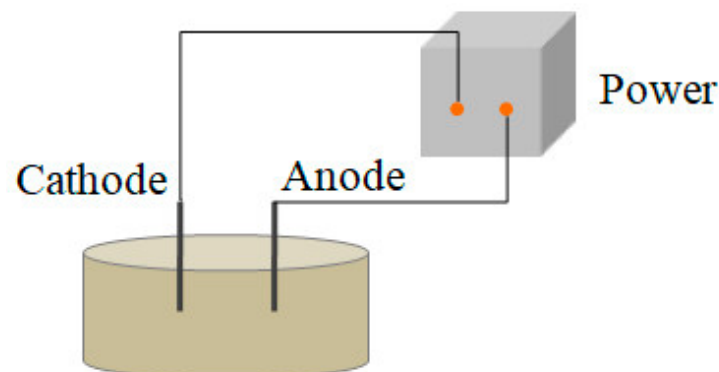


Figure 16. Schematic diagram of electrochemical deposition method.

The comparison of the above preparation methods of high-entropy alloys is shown in Table 2.

Table 2. Comparison of preparation methods of high-entropy alloys.

Preparation Methods	Characteristics
Melting-casting method	The melting temperature is high, and it can be melted many times. The melt is mixed evenly, and the low melting point impurities are volatile.
Mechanical alloying method	The particle size can be controlled and the mechanical properties can be effectively controlled.
Laser cladding	It can rapidly solidify, inhibit the precipitation of intermetallic compounds and promote the nucleation of solid solution.
Magnetron sputtering	The sputtering power can affect the grain size, change the film composition and control the film thickness.
Thermal spray technology	The coating is dense and smooth, the mechanical occlusion between the coating and the substrate is good and the interface bonding is good.
Electrochemical deposition method	The structure of the deposited layer can be accurately controlled, the equipment is simple, the energy consumption is low and the operation is easy.

5. Properties of High-Entropy Alloys

The unique formation rule and microstructure characteristics of high-entropy alloys determine that high-entropy alloys have better performance than other traditional alloys. These good comprehensive properties give high-entropy alloys great application prospects in aerospace, machinery manufacturing, metallurgy, chemical industry and other fields [68–70].

5.1. Strength and Toughness

The mechanical properties are the most studied for high-entropy alloys. This is because the high mixing entropy makes them tend to form simple solid solution phases. The strength and toughness of high-entropy alloys can be well matched, and their mechanical properties are better than most traditional alloys [71].

A variety of strengthening mechanisms are stimulated by adjusting the microstructure and machining to improve the properties of high-entropy alloys. Xiao et al. [72] prepared a kind of high-entropy alloy, and the hardness of the alloy was as high as 13.76 GPa. Yang et al. [73] synthesized $\text{Ni}_{43.9}\text{Co}_{22.4}\text{Fe}_{8.8}\text{Al}_{10.7}\text{Ti}_{11.7}\text{B}_{2.5}$ alloys by arc melting and thermomechanical processing. The strength and elongation at room temperature are as high as 1.6 GPa and 25%, respectively. Gludovatz et al. [74] studied CrMnFeCoNi alloys with a tensile strength of more than 1 GPa and a fracture toughness value of more than $200 \text{ MPa}\cdot\text{m}^{1/2}$, which is higher than most materials, as shown in Figure 17, when the temperature drops to liquid nitrogen.

5.2. Wear Resistance

Tribological properties are very important in engineering, especially for moving workpieces such as bearings and gears. Due to the influence of the use environment, it is necessary to meet the strength requirements and consider the service life, so the tribological performance requirements of materials are also crucial. Zeng et al. [75] prepared AlFeCrNiMo coatings on 304 stainless steel. Because Al and Cr metals in the high-entropy alloy coatings are prone to oxidation reactions which form Cr_2O_3 and Al_2O_3 layers, the oxidation products produced play an important role in the formation of lubricity film and have good wear resistance. Chuang et al. [76] prepared $\text{Al}_x\text{Co}_{1.5}\text{CrFeNi}_{1.5}\text{Ti}_y$ alloys and found that the wear resistance of this alloy is better than that of traditional wear-resistant steel with similar hardness. The reason for the improved wear resistance is that the alloy

has oxidation resistance and high temperature softening resistance. Figure 18 shows the relationship between microhardness and friction resistance of several high-entropy alloys and traditional alloys.

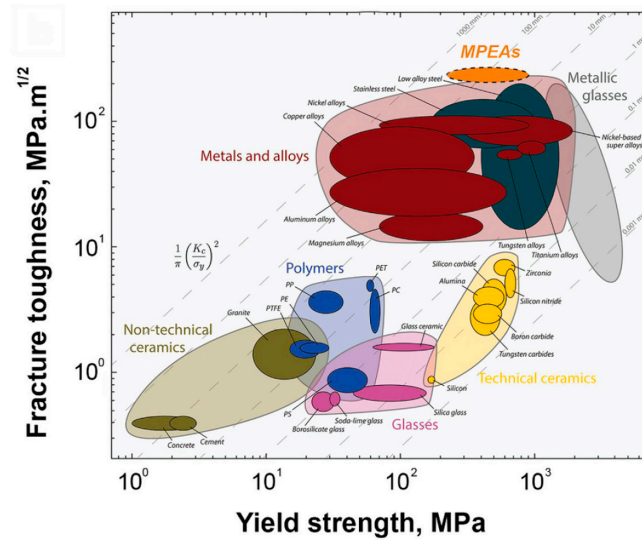


Figure 17. Comparison of fracture toughness and yield strength between high-entropy alloys and other materials [74].

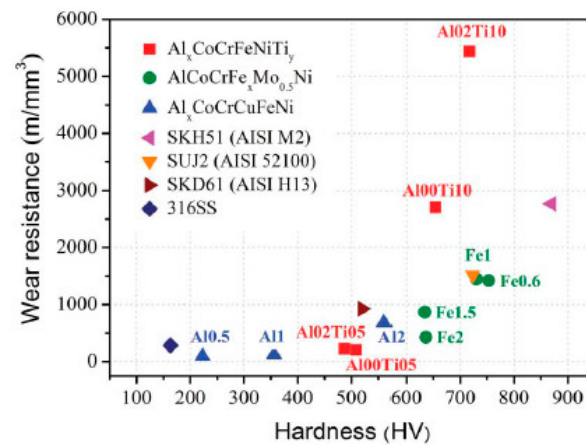


Figure 18. Comparison between wear resistance and hardness of various alloys [23].

5.3. Corrosion Resistance

Most of the principal elements of the high-entropy alloys have corrosion resistance, such as metal Ni, Cr, Mo, Al, Cu and so on. Some of these elements form passivation films by themselves, or interact with each other to form a dense composite passivation film, so as to improve the corrosion resistance of the alloy in acid, alkali, salt and other corrosive environments. In addition, the crystal structure is relatively simple, can easily form single-phase solid solution or amorphous phase and can obtain excellent corrosion resistance comparable to 304 stainless steel or amorphous alloys. The $Hf_{0.5}Nb_{0.5}Ta_{0.5}Ti_{1.5}Zr$ alloy designed by Hou et al. [77] has excellent corrosion resistance. Xiao et al. [78] found that the addition of Cr can improve the corrosion resistance of alloys, and Cr can easily form Cr_2O_3 to prevent high-entropy alloys from being corroded at room temperature. Zhang et al. [79] studied the electrochemical corrosion properties of FeCoNiCrCu high-entropy alloy coatings containing small amounts of Si, Mn and Mo. The results show that the coatings have excellent electrochemical corrosion resistance.

5.4. High Temperature Resistance

One of the important properties of high-entropy alloys different from other traditional alloys is high temperature resistance. Table 3 shows the comparison between the high-entropy alloys and the conventional alloys in the as-cast and annealed states [7]. After annealing at 1000 °C for 12 h, the high-entropy alloys still maintain a high hardness, and some high-entropy alloys will even increase in hardness. However, the hardness values of many traditional alloys decreased significantly after annealing.

Table 3. Comparison between the high-entropy alloys and the conventional alloys in two states [7].

Alloys	Hardness, HV As-Cast	Hardness, HV Annealed
CuTiVFeNiZr	590	600
AlTiVFeNiZr	800	790
MoTiVFeNiZr	740	760
CuTiVFeNiZrCo	630	620
AlTiVFeNiZrCo	790	800
MoTiVFeNiZrCo	790	790
CuTiVFeNiZrCoCr	680	680
AlTiVFeNiZrCoCr	780	890
MoTiVFeNiZrCoCr	850	850
316 Stainless Steel	189	155
17-4 PH Stainless Steel	410	362
Hastelloy C	236	280
Stellite 6	413	494
Ti-6Al-4V	412	341

Grewal et al. [80] compared the oxidation resistance of $Al_{0.1}CoCrFeNi$ alloys with commonly used steel alloys and coatings at 1173 K, and found that the formation of Cr_2O_3 protective film by Cr and slow diffusion effect meant that the $Al_{0.1}CoCrFeNi$ alloy has better high temperature oxidation resistance. Lu et al. [81] found that with the increase in aluminum content, the alloys showed an extremely slow oxidation rate and good high temperature oxidation resistance. Senkov et al. [82] studied the oxidation behavior of $NbCrMo_{0.5}Ta_{0.5}TiZr$ alloys exposed to air at 1273 K for 100 h. The results showed that the alloys have better oxidation resistance than other alloys such as the Nb alloy.

5.5. Fatigue Resistance

Hemphill et al. [83] studied the fatigue properties of $Al_{0.5}CoCrCuFeNi$ high-entropy alloys, and the results are shown in Figure 19. It can be seen that the high-entropy alloys have excellent fatigue resistance compared with other traditional alloys. Moreover, under high stress state, the $Al_{0.5}CoCrCuFeNi$ high-entropy alloys have a longer cycle fatigue life between 540 MPa and 945 MPa, and the ratio of fatigue life to fracture strength is between 0.402 and 0.703. This phenomenon can be comparable to the fatigue properties of traditional alloys such as steel materials and Ti alloys.

5.6. Radiation Resistance

With the continuous development of nuclear technology, both the power generation equipment of nuclear power plants and the equipment for processing nuclear waste in power plants need materials that can serve safely in a high radiation environment for a long time. Therefore, improving the radiation resistance of materials plays an important role in the development of nuclear technology. Studies have shown that high-entropy alloys still have certain stability under radiation. Taking $NiCoFeCrMn$ as the research object, Su et al. [84] changed the chemical heterogeneities by adding nitrogen and carbon atoms. The results showed that are duction in void swelling by at least one order of magnitude. Deluigi et al. [85] used molecular dynamics to conclude that the reason for the radiation resistance of high-entropy alloys may be caused by the evolution of defects for a long

time. Li et al. [86] studied the chemical ordering effect on the radiation resistance, and obtained a radiation repair model. Orhan et al. [87] studied the electronic properties of random solid solutions, and found that adding lighter elements can improve the radiation resistance of high-entropy alloys. These studies have opened up a promising way for high radiation-resistant alloys.

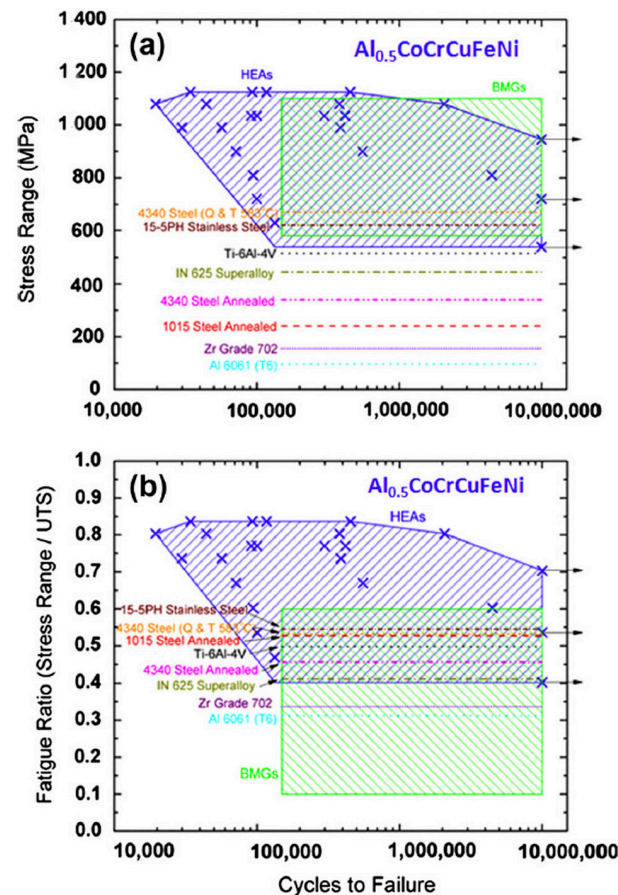


Figure 19. Comparison between fatigue property and stress range of alloys [83].

5.7. Magnetic Properties

In addition to excellent mechanical properties, the high-entropy alloys also have good physical properties. As the main ferromagnetic elements, Fe, Co and Ni can give high-entropy alloys excellent magnetic properties through reasonable composition design [88]. Gao et al. [89] researched a new CoFeAlMn high-entropy alloy with satisfied magnetic properties. Studies have shown that a few high-entropy alloys can exhibit hard magnetic properties. Feng et al. [90] studied the hard magnetic properties of high-entropy alloys. The $Nd_{20}Pr_{20}La_{20}Fe_{20}Co_{10}Al_{10}$ high-entropy alloy is designed. Duan et al. [91] developed a novel $(Fe_{2.25}Co_{1.25}Cr)_{94}Al_6$ high-entropy alloy. The soft magnetic properties are superior to other reported alloys. These findings provide a new way for the development of magnetic properties of high-entropy alloys to widen their applications.

In addition to the above performance, Wang et al. [92] studied the $(Ni_{40}Fe_{30}Co_{20}Al_{10})_{90}Ti_{10}$ high-entropy alloy. The high-entropy alloy powder after grinding showed superior photocatalytic performance. Wu et al. [93] proposed the high-entropy alloy $(FeCoNiCuZn)WO_4$ which can grow on polyacrylonitrile nanofiber templates. The high-entropy photocatalyst fiber membrane was reported. Wail et al. [94] studied a strategy for synthesizing stable high-entropy alloy nanoparticles.

A nanocomposite material is given in [94]. Compared with the high-entropy alloys prepared in [89,91], the magnetic properties are much smaller than the latter two, but the

coercivity is significantly increased. It is often used in the biomedical field. In general, compared with high-entropy alloy materials, nanomaterials usually have larger specific surface area, smaller size, high surface activity and strong controllability. However, the production cost is generally higher, and their stability is relatively poor due to the high surface activity.

6. Summary and Outlook

As a new type of material, high-entropy alloys have developed rapidly in the field of metal materials in recent years and have important academic value and broad application prospects. High-entropy alloys can be designed according to different performance requirements because of their excellent properties. High-entropy alloys have good mechanical, thermal and magnetic properties, which give them broad application prospects in mold manufacturing, catalytic materials, aerospace, surface engineering, anti-radiation materials and other fields.

At present, the research of high-entropy alloys is still in a preliminary exploration stage, and there are many problems to be solved. There is still a lack of a new and more scientific theoretical guidance system for the research of high-entropy alloys. Whether it is to use the existing alloy research methods such as phase diagram to analyze and speculate on the relationship between its composition, structure and properties, or to select and repeatedly test the alloy composition through the cocktail effect, it has a certain blindness. How to further improve the efficiency of high-entropy alloys research with modeling and simulation technology scientifically and reasonably is one of the key contents to be studied next. The properties of high-entropy alloys are still limited under special circumstances. At present, there are relatively few studies on the properties under extreme conditions and some special properties, and in-depth research will broaden the application prospects of high-entropy alloys. Although a series of high-entropy alloys can be obtained through various preparation methods, there are limitations in various methods, such as uneven particle size distribution, low accuracy of component content control and low yield under extreme synthesis conditions. It is necessary to further improve or develop new preparation techniques and optimize the synthesis strategy. The application of material characterization technology is the key to discover, confirm and analyze the composition, structure and properties of high-entropy alloys. Therefore, how to effectively realize the coupling between characterization information and material properties, and use advanced characterization techniques to establish and analyze the structure-activity relationship between high-entropy structure and its properties is also one of the key contents to be studied next. There are still a lot of functional properties of high-entropy alloy nanoparticles to be developed, and the related performance mechanism needs to be analyzed. The application of artificial intelligence and big data technology in the preparation process and industrial production of high-entropy alloys and the further development of automatic, intelligent and integrated high-entropy alloy preparation technology can further promote the industrialization of high-entropy alloys.

Author Contributions: Data curation, S.Z.; methodology, S.Z.; writing—original draft, Z.W. All authors have read and agreed to the published version of the manuscript.

Funding: This work was supported by Research funding of Talent Introduction Program of Liaoning Technical University (552305900128).

Institutional Review Board Statement: Not applicable.

Informed Consent Statement: Not applicable.

Data Availability Statement: Data are contained within the article.

Conflicts of Interest: The authors declare no conflict of interest.

References

1. Lim, X.Z. Mixed-up metals make for stronger, tougher, stretchier alloys. *Nature* **2016**, *533*, 306–307. [[CrossRef](#)] [[PubMed](#)]

2. Li, T.X.; Wang, S.D.; Lu, Y.P.; Cao, Z.Q.; Wang, T.M.; Li, T.J. Research Progress and Prospect of High-Entropy Alloy Materials. *Chin. Eng. Sci.* **2023**, *25*, 170–181. [[CrossRef](#)]
3. Cantor, B.; Kim, K.B.; Warren, P.J. Novel multicomponent amorphous alloys. *J. Metastable Nanocrystalline Mater.* **2002**, *13*, 27–32. [[CrossRef](#)]
4. Cantor, B.; Chang, I.T.H.; Knight, P.; Vincent, A.J.B. Microstructural development in equiatomic multicomponent alloys. *Mater. Sci. Eng. A* **2004**, *375–377*, 213–218. [[CrossRef](#)]
5. Zhang, Y.; Zuo, T.T.; Tang, Z.; Michael, C.G.; Karin, A.D.; Peter, K.L.; Zhao, P.L. Microstructures and properties of high-entropy alloys. *Prog. Mater. Sci.* **2014**, *61*, 1–93. [[CrossRef](#)]
6. Yeh, J.W.; Su, J.L.; Chin, T.S.; Gan, J.Y.; Chen, S.W.; Shun, T.T.; Tsau, C.H.; Chou, S.Y. Formation of simple crystal structures in Cu-Co-Ni-Cr-Al-Fe-Ti-Alloys with multiprincipal metallic elements. *Metall. Mater. Trans. A* **2004**, *35*, 2533–2536. [[CrossRef](#)]
7. Yeh, J.W.; Chen, S.K.; Lin, S.J.; Gan, J.Y.; Chin, T.S.; Shun, T.T.; Tsau, C.H.; Chang, S.Y. Nanostructured high-entropy alloys with multiple principal elements novel alloy design concepts and outcomes. *Adv. Eng. Mater.* **2004**, *6*, 299–303. [[CrossRef](#)]
8. Sharma, P.; Dwivedi, V.K.; Dwivedi, S.P. Development of high entropy alloys: A review. *Mater. Today* **2021**, *43*, 502–509. [[CrossRef](#)]
9. Ikeuchi, D.; King, D.J.M.; Laws, K.J.; Knowles, A.J.; Aughterson, R.D.; Lumpkin, G.R.; Obbard, E.G. Cr-Mo-V-W: A new refractory and transition metal high-entropy alloy system. *Scripta Mater.* **2019**, *158*, 141–145. [[CrossRef](#)]
10. Wei, Q.Q.; Shen, Q.; Zhang, J.; Chen, B.; Luo, G.Q.; Zhang, L.M. Microstructure and mechanical property of a novel ReMoTaW high-entropy alloy with high density. *Int. J. Refract. Meth.* **2018**, *77*, 8–11. [[CrossRef](#)]
11. Chaudhary, V.; Gwalani, B.; Soni, V.; Ramanujan, R.V.; Banerjee, R. Influence of Cr substitution and temperature on hierarchical-phase decomposition in the AlCoFeNi high entropy alloy. *Sci. Rep.* **2018**, *8*, 15578. [[CrossRef](#)] [[PubMed](#)]
12. Coury, F.G.; Butler, T.; Chaput, K.; Saville, A.; Copley, J.; Foltz, J.; Mason, P.; Clarke, K.; Kaufman, M.; Clarke, A. Phase equilibria, mechanical properties and design of quaternary refractory high entropy alloys. *Mater. Des.* **2018**, *155*, 244–256. [[CrossRef](#)]
13. Liao, M.Q.; Liu, Y.; Min, L.J.; Lai, Z.H.; Han, T.Y.; Yang, D.N.; Zhu, J.C. Alloying effect on phase stability, elastic and thermodynamic properties of Nb-Ti-V-Zr high entropy alloy. *Intermetallics* **2018**, *101*, 152–164. [[CrossRef](#)]
14. Ding, J.; Asta, M.; Ritchie, R.O. Melts of CrCoNi-based high-entropy alloys: Atomic diffusion and electronic/atomic structure from ab initio simulation. *Appl. Phys. Lett.* **2018**, *113*, 111902. [[CrossRef](#)]
15. Yeh, J.W. Recent progress in high entropy alloys. *Ann. Chim. Sci. Mat.* **2006**, *31*, 633–648. [[CrossRef](#)]
16. Tong, C.J.; Chen, M.R.; Chen, S.K. Mechanical performance of the Al_xCoCrCuFeNi high-entropy alloy system with multiprincipal elements. *Metall. Mater. Trans. A* **2005**, *36A*, 1263–1271. [[CrossRef](#)]
17. Tong, C.J.; Chen, Y.L.; Chen, S.K. Microstructure characterization of Al_xCoCrCuFeNi high-entropy alloy system with multiprincipal elements. *Metall. Mater. Trans. A* **2005**, *36A*, 881–893. [[CrossRef](#)]
18. Li, A.; Zhang, X. Thermodynamic analysis of the simple microstructure of AlCrFeNiCu high-entropy alloy with multi-principal elements. *Acta Metall. Sin.* **2009**, *22*, 219–224. [[CrossRef](#)]
19. Senkov, O.N.; Wilks, G.B.; Miracle, D.B.; Chuang, C.P.; Liaw, P.K. Refractory high-entropy alloys. *Intermetallics* **2010**, *18*, 1758–1765. [[CrossRef](#)]
20. Del, G.M.F.; Bozzolo, G.; Hugo, O.M. Determination of the transition to the high entropy regime for alloys of refractory elements. *J. Alloys Compd.* **2012**, *534*, 25–31.
21. Ng, C.; Guo, S.; Luan, J.; Shi, S.; Liu, C.T. Entropy-driven phase stability and slow diffusion kinetics in an Al_{0.5}CoCrCuFeNi high entropy alloy. *Intermetallics* **2012**, *31*, 165–171. [[CrossRef](#)]
22. Lucas, M.S.; Wilks, G.B.; Mauger, L.; Munoz, J.A.; Karapetrova, E. Absence of long-range chemical ordering in equimolar FeCoCrNi. *Appl. Phys. Lett.* **2012**, *100*, 251907-1–251907-4. [[CrossRef](#)]
23. Tsai, M.H.; Yeh, J.W. High-Entropy Alloys: A Critical Review. *Mater. Res. Lett.* **2014**, *2*, 107–123. [[CrossRef](#)]
24. Yeh, J.W.; Chang, S.Y.; Hong, Y.D.; Chen, S.K.; Lin, S.J. Anomalous decrease in X-ray diffraction intensities of CuNiAlCoCrFeSi alloy systems with multi-principal elements. *Mater. Chem. Phys.* **2007**, *103*, 41–46. [[CrossRef](#)]
25. Tsai, M.H. Physical Properties of high entropy alloys. *Entropy* **2013**, *15*, 5338–5345. [[CrossRef](#)]
26. Tsai, K.Y.; Tsai, M.H.; Yeh, J.W. Sluggish diffusion in Co–Cr–Fe–Mn–Ni high-entropy alloys. *Acta. Mater.* **2013**, *61*, 4887–4897. [[CrossRef](#)]
27. Kottke, J.; Laurent-Brocq, M.; Fareed, A.; Wilde, G. Tracer diffusion in the Ni-CoCrFeMn system: Transition from a dilute solid solution to a high entropy alloy. *Scripta Mater.* **2019**, *159*, 94–98. [[CrossRef](#)]
28. Chen, W.Y.; Liu, X.; Chen, Y.R.; Yeh, J.W.; Tseng, K.K.; Natesan, K. Irradiation effects in high entropy alloys and 316H stainless steel at 300 degrees C. *J. Nucl. Mater.* **2018**, *510*, 421–430. [[CrossRef](#)]
29. Wang, R.; Chen, W.M.; Zhong, J.; Zhang, L. Experimental and numerical studies on the sluggish diffusion in face centered cubic Co-Cr-Cu-Fe-Ni high-entropy alloys. *J. Mater. Sci. Technol.* **2018**, *34*, 1791–1798. [[CrossRef](#)]
30. Vaidya, M.; Trubel, S.; Murty, B.S.; Wilde, G.; Divinski, S.V. Ni tracer diffusion in CoCrFeNi and CoCrFeMnNi high entropy alloys. *J. Alloys Compd.* **2016**, *688*, 994–1001. [[CrossRef](#)]
31. Dąbrowa, J.; Kucza, W.; Cieślak, G.; Kulik, T.; Danielewski, M.; Yeh, J.W. Interdiffusion in the FCC-structured Al-Co-Cr-Fe-Ni high entropy alloys: Experimental studies and numerical simulations. *J. Alloys Compd.* **2016**, *674*, 455–462. [[CrossRef](#)]
32. Yang, M.; Liu, X.J.; Ruan, H.H.; Wu, Y.; Wang, H.; Lu, Z.P. High thermal stability and sluggish crystallization kinetics of high-entropy bulk metallic glasses. *J. Appl. Phys.* **2016**, *119*, 245112. [[CrossRef](#)]
33. Ranganathan, S. Alloyed pleasures: Multimetallurgical cocktails. *Curr. Sci.* **2003**, *85*, 1404–1406.

34. Sanchez, J.M.; Vicario, I.; Albizuri, J.; Guraya, T.; Garcia, J.C. Phase prediction, microstructure and high hardness of novel light-weight high entropy alloys. *J. Mater. Res. Technol.* **2019**, *8*, 795–803. [[CrossRef](#)]
35. Huang, D.; Lu, J.; Zhuang, Y.; Tian, C.; Li, Y. The role of Nb on the high temperature oxidation behavior of CoCrFeMnNb_xNi high-entropy alloys. *Corros. Sci.* **2019**, *158*, 108088.1–108088.9. [[CrossRef](#)]
36. Gwalani, B.; Choudhuri, D.; Soni, V.; Ren, Y.; Styles, M.; Hwang, J.Y.; Nam, S.J.; Ryu, H.; Hong, S.H.; Banerjee, R. Cu assisted stabilization and nucleation of L12 precipitates in Al_{0.3}CuFeCrNi₂fcc-based high entropy alloy. *Acta Mater.* **2017**, *129*, 170–182. [[CrossRef](#)]
37. Sun, H.F.; Guo, N.; Wang, C.M.; Li, Z.L.; Zhu, H.Y. Study of the microstructure of high-entropy alloys AlFeCuCoNiCrTi_x. *Appl. Mech. Mater.* **2011**, *66*, 894–900. [[CrossRef](#)]
38. Li, C.; Li, J.C.; Zhao, M.; Jiang, Q. Effect of alloying elements on microstructure and properties of multiprincipal elements high-entropy alloys. *J. Alloys Compd.* **2009**, *475*, 752–757. [[CrossRef](#)]
39. Hu, Z.; Zhan, Y.; Zhang, G.; She, J.; Li, C. Effect of rare earth Y addition on the microstructure and mechanical properties of high entropy AlCoCrCuNiTi alloys. *Mater. Des.* **2010**, *31*, 1599–1602. [[CrossRef](#)]
40. Wen, L.H.; Kou, H.C.; Li, J.S.; Chang, H.; Xue, X.Y.; Zhou, L. Effect of aging temperature on microstructure and properties of AlCoCrCuFeNi high-entropy alloy. *Intermetallics* **2009**, *17*, 266–269. [[CrossRef](#)]
41. Fang, S.; Chen, W.; Fu, Z. Microstructure and mechanical properties of twinned Al_{0.5}CrFeNiCo_{0.3}Co_{0.2} high entropy alloy processed by mechanical alloying and spark plasma sintering. *Mater. Des.* **2014**, *54*, 973–979. [[CrossRef](#)]
42. Cai, Z.; Jin, G.; Cui, X.; Yang, L.; Yang, F.; Song, J. Experimental and simulated data about microstructure and phase composition of a NiCrCoTiV high-entropy alloy prepared by vacuum hot-pressing sintering. *Vacuum* **2016**, *124*, 5–10. [[CrossRef](#)]
43. Braeckman, B.R.; Depla, D. Structure formation and properties of sputter deposited Nb_x-CoCrCuFeNi high entropy alloy thin films. *J. Alloys Compd.* **2015**, *646*, 810–815. [[CrossRef](#)]
44. Zhang, H.; Wu, W.; He, Y.; Li, M.; Guo, S. Formation of core-shell structure in high entropy alloy coating by laser cladding. *Appl. Surf. Sci.* **2016**, *363*, 543–547. [[CrossRef](#)]
45. An, Z.N.; Jia, H.; Wu, Y.; Rack, P.D.; Patchen, A.D.; Liu, Y.; Yang, R.; Li, N.; Liaw, P.K. Solid-solution CrCoCuFeNi high-entropy alloy thin films synthesized by sputter deposition. *Mater. Res. Lett.* **2015**, *3*, 203–209. [[CrossRef](#)]
46. Zhou, Y.J.; Zhang, Y.; Wang, Y.L. Microstructure and compressive properties of multicomponent Al_x(TiVCrMnFeCoNiCu)_(100-x) high-entropy alloys. *Mater. Sci. Eng. A* **2007**, *454/455*, 260–265. [[CrossRef](#)]
47. Fujieda, J.D.; Shiratori, H.; Kuwabara, K.; Kato, T.; Yamanaka, K.; Koizumi, Y.; Chiba, A. First demonstration of promising selective electron beam melting method for utilizing high-entropy alloys as engineering materials. *Mater. Lett.* **2015**, *159*, 12–15. [[CrossRef](#)]
48. Varalakshmi, S.; Kamaraj, M.; Murty, B.S. Synthesis and characterization of nanocrystal line AlFeTiCrZnCu high entropy solid solution by mechanical alloying. *J. Alloys Compd.* **2008**, *460*, 253–257. [[CrossRef](#)]
49. Zhang, G.J.; Tian, Q.W.; Yin, K.X.; Niu, S.Q.; Wu, M.H.; Wang, W.W.; Huang, J.C. Effect of Fe on microstructure and properties of AlCoCrFexNi(x=1.5, 2.5) high entropy alloy coatings prepared by laser cladding. *Intermetallics* **2020**, *119*, 106722. [[CrossRef](#)]
50. Chang, F.; Cai, B.J.; Zhang, C.; Huang, B.; Li, S.; Dai, P.Q. Thermal stability and oxidation resistance of FeCr_xCoNiB high-entropy alloys coatings by laser cladding. *Surf. Coat. Technol.* **2019**, *359*, 132–140. [[CrossRef](#)]
51. Huang, C.; Zhang, Y.Z.; Rui, V.; Shen, J.Y. Dry sliding wear behavior of laser clad TiVCrAlSi high entropy alloy coatings on Ti-6Al-4V substrate. *Surf. Coat. Technol.* **2012**, *41*, 338–343. [[CrossRef](#)]
52. Jiang, Y.Q.; Li, J.; Juan, Y.F.; Lu, Z.J.; Jia, W.L. Evolution in microstructure and corrosion behavior of AlCoCr_xFeNi high-entropy alloy coatings fabricated by laser cladding. *J. Alloys Compd.* **2019**, *775*, 1–14. [[CrossRef](#)]
53. Liu, J.; Liu, H.; Chen, P.J.; Hao, J.B. Micro structure characterization and corrosion behavior of AlCoCrFeNiTi_x high-entropy alloy coatings fabricated by laser cladding. *Surf. Coat. Technol.* **2019**, *361*, 36–74. [[CrossRef](#)]
54. Chen, T.K.; Shun, T.T.; Yeh, J.W.; Wong, M.S. Nanostructured nitride films of multi-element high-entropy alloys by reactive DC sputtering. *Surf. Coat. Technol.* **2004**, *188*, 193–200. [[CrossRef](#)]
55. Chang, Z.C.; Liang, S.C.; Han, S.; Chen, Y.K.; Sheiu, F.S. Characteristics of TiVCrAlZr multi-element nitride film sprepared by reactive sputtering. *Nucl. Instrum. Meth. A* **2010**, *268*, 2504–2509. [[CrossRef](#)]
56. Lin, C.H.; Duh, J.G.; Yeh, J.W. Multi-component nitride coatings derived from Ti-Al-Cr-Si-V target in RF magnetron sputter. *Surf. Coat. Technol.* **2007**, *201*, 6304–6308. [[CrossRef](#)]
57. Huang, P.K.; Yeh, J.W. Effects of substrate temperature and post-annealing on microstructure and properties of (AlCrNbSiTiV)N coatings. *Thin Solid Films* **2009**, *518*, 180–184. [[CrossRef](#)]
58. Chang, H.W.; Huang, P.K.; Yeh, J.W.; Davison, A.; Tsau, C.H.; Yang, C.C. Influence of substrate bias, deposition temperature and post-deposition annealing on the structure and properties of multi-principal-component (AlCrMoSiTi)N coatings. *Surf. Coat. Technol.* **2008**, *202*, 3360–3366. [[CrossRef](#)]
59. Ran, C.A.B.; Cai, Z.B.; Pu, J.B.; Lu, Z.X.; Chen, S.Y.; Zheng, S.J.; Zeng, C. Effects of nitriding on the microstructure and properties of VAlTiCrMo high-entropy alloy coatings by sputtering technique. *J. Alloys Compd.* **2020**, *827*, 153836.
60. Huo, W.Y.; Liu, X.D.; Tan, S.Y.; Feng, F.; Xie, Z.H. Ultrahigh hardness and high electrical resistivity in nano-twinned, nanocrystalline high-entropy alloy films. *Appl. Surf. Sci.* **2018**, *439*, 222–225. [[CrossRef](#)]
61. Huang, P.K.; Yeh, J.W.; Shun, T.T.; Chen, S.K. Multi-principal-element alloys with improved oxidation and wear resistance for thermal spray coating. *Adv. Eng. Mater.* **2004**, *6*, 74–78. [[CrossRef](#)]

62. Ang, A.S.M.; Berndt, C.C.; Sesso, M.L.; Anupam, A.; Kottada, R.S.; Murty, B.S. Plasma-sprayed high entropy alloys: Microstructure and properties of AlCoCrFeNi and MnCoCrFeNi. *Metall. Mater. Trans. A* **2015**, *46*, 791–800. [[CrossRef](#)]
63. Wang, C.; Yu, J.; Zhang, Y.; Yu, Y. Phase evolution and solidification cracking sensibility in laser remelting treatment of the plasma-sprayed CrMnFeCoNi high entropy alloy coating. *Mater. Des.* **2019**, *182*, 108040. [[CrossRef](#)]
64. Chen, L.J.; Bobzin, K.; Zhou, Z.; Zhao, L.; Te, M.; Knigstein, T.; Tan, Z.; He, D. Wear behavior of HVOF-sprayed Al_{0.6}TiCrFeCoNi high entropy alloy coatings at different temperatures. *Surf. Coat. Technol.* **2019**, *358*, 215–222. [[CrossRef](#)]
65. Yao, C.Z.; Peng, L.; Li, G.R.; Ye, J.Q.; Peng, L.; Tong, Y.X. Electrochemical preparation and magnetic study of Bi-Fe-Co-Ni-Mn high entropy alloy. *Electrochim. Acta* **2008**, *53*, 8359–8365. [[CrossRef](#)]
66. Soare, V.; Burada, M.; Constantin, I.; Mitrica, D.; Badilita, V.; Caragea, A.; Tarcolea, M. Electrochemical deposition and microstructural characterization of AlCrFeMnNi and AlCrCuFeMnNi high entropy alloy thin films. *Appl. Surf. Sci.* **2015**, *358*, 533–539. [[CrossRef](#)]
67. Ahmed, A.; Chandan, S. Microstructure and corrosion performance of AlFeCoNiCu high entropy alloy coatings by addition of grapheme oxide. *Materialia* **2019**, *8*, 100459.
68. Wang, X.R.; Wang, Z.Q.; He, P.; Wang, Z.Q.; Shi, Y. Microstructure and wear properties of CuNiSiTiZr high-entropy alloy coatings on TC11 titanium alloy produced by electrospark-computer numerical control deposition process. *Surf. Coat. Technol.* **2015**, *283*, 156–161. [[CrossRef](#)]
69. Zhang, Y.; Wang, Z.; Qiao, H.; Yang, H. Microstructural features and tensile behaviors of the Al_{0.5}CrCuFeNi₂ high-entropy alloys by cold rolling and subsequent annealing. *Mater. Des.* **2015**, *88*, 1057–1062.
70. Raza, A.; Ryu, H.J.; Hong, S.H. Strength enhancement and density reduction by the addition of Al in CrFeMoV based high-entropy alloy fabricated through powder metallurgy. *Mater. Des.* **2018**, *157*, 97–104. [[CrossRef](#)]
71. Ye, Y.F.; Wang, Q.; Lu, J.; Liu, C.T.; Yang, Y. High-entropy alloy: Challenges and prospects. *Mater. Today* **2016**, *19*, 349–362. [[CrossRef](#)]
72. Xiao, L.L.; Zheng, Z.Q.; Guo, S.W.; Huang, P.; Wang, F. Ultra-strong nanostructured CrMnFeCoNi high entropy alloys. *Mater. Des.* **2020**, *194*, 108895. [[CrossRef](#)]
73. Yang, T.; Zhao, Y.L.; Li, W.P.; Yu, C.Y.; Luan, J.H.; Lin, D.Y.; Fan, L.; Jiao, Z.B.; Liu, W.H.; Liu, X.J. Ultrahigh-strength and ductile superlattice alloys with nanoscale disordered interfaces. *Science* **2020**, *369*, 427–432. [[CrossRef](#)]
74. Gludovatz, B.; Hohenwarter, A.; Catoor, D.; Chang, E.H.; George, E.P.; Ritchie, R. A fracture-resistant high-entropy alloy for cryogenic applications. *Science* **2014**, *345*, 1153–1158. [[CrossRef](#)]
75. Zeng, Q.F.; Xu, Y.T. A comparative study on the tribocorrosion behaviors of AlFeCrNiMo high entropy alloy coatings and 304 stainless steel. *Mater. Today Commun.* **2020**, *24*, 101261. [[CrossRef](#)]
76. Chuang, M.H.; Tsai, M.H.; Wang, W.R.; Lin, S.J.; Yeh, J.W. Microstructure and wear behavior of Al_xCo_{1.5}CrFeNi_{1.5}Ti_y high-entropy alloys. *Acta Mater.* **2011**, *59*, 6308–6317. [[CrossRef](#)]
77. Zhou, Q.Y.; Sheikh, S.; Ou, P. Corrosion behavior of Hf_{0.5}Nb_{0.5}Ta_{0.5}Ti_{1.5}Zr refractory high-entropy in aqueous chloride solutions. *Electrochem. Commun.* **2019**, *98*, 63–68. [[CrossRef](#)]
78. Xiao, D.H.; Zhou, P.F.; Wu, W.Q.; Diao, H.Y.; Gao, M.C.; Song, M.; Liaw, P.K. Microstructure, mechanical and corrosion behaviors of AlCoCuFeNi-(Cr, Ti) high entropy alloys. *Mater. Des.* **2017**, *116*, 438–447. [[CrossRef](#)]
79. Zhang, H.; Pan, Y.; He, Y.Z. Synthesis and characterization of FeCoNiCrCu high-entropy alloy coating by laser cladding. *Mater. Des.* **2011**, *32*, 1910–1915. [[CrossRef](#)]
80. Grewal, H.S.; Sanjiv, R.M.; Arora, H.S.; Kumar, R.; Singh, H. Activation energy and high temperature oxidation behavior of multi-principal element alloy. *Adv. Eng. Mater.* **2017**, *19*, 1700182. [[CrossRef](#)]
81. Lu, J.; Chen, Y.; Zhang, H.; Li, L.; Xiao, P. Effect of Al content on the oxidation behavior of Y/Hf-doped AlCoCrFeNi high-entropy alloy. *Corros. Sci.* **2020**, *170*, 108691. [[CrossRef](#)]
82. Senkov, O.N.; Senkova, S.V.; Dimiduk, D.M.; Woodward, C.; Senkov, O.N. Oxidation behavior of a refractory NbCrMo_{0.5}Ta_{0.5}TiZr alloy. *J. Mater. Sci.* **2012**, *47*, 6522–6534. [[CrossRef](#)]
83. Hemphill, M.A.; Yuan, T.; Wang, G.Y.; Yeh, J.W.; Tsai, C.W.; Chuang, A.; Liaw, P.K. Fatigue behavior of Al_{0.5}CoCrCuFeNi high entropy alloys. *Acta Mater.* **2012**, *60*, 5723–5734. [[CrossRef](#)]
84. Su, Z.X.; Ding, J.; Song, M.; Jiang, L.; Shi, T.; Li, Z.; Wang, S.; Gao, F.; Yun, D.; Ma, E.; et al. Enhancing the radiation tolerance of high-entropy alloys via atomic-scale chemical heterogeneities. *Acta Mater.* **2023**, *245*, 118662. [[CrossRef](#)]
85. Deluigi, O.R.; Pasianot, R.C.; Valencia, F.J.; Caro, A.; Bringa, E.M. Simulations of primary damage in a high entropy alloy: Probing enhanced radiation resistance. *Acta Mater.* **2021**, *213*, 116951. [[CrossRef](#)]
86. Li, Y.G.; Du, J.P.; Yu, P.J.; Li, R.; Shinzato, S.H.; Peng, Q.; Ogata, S. Chemical ordering effect on the radiation resistance of a CoNiCrFeMn high-entropy alloy. *Comput. Mater.* **2022**, *214*, 111764. [[CrossRef](#)]
87. Orhan, O.K.; Hendy, M.; Ponga, M. Electronic effects on the radiation damage in high-entropy alloys. *Acta Mater.* **2023**, *244*, 118511. [[CrossRef](#)]
88. Zeng, C.; He, W.; Ai, Y.L.; Chen, W.H.; Liang, B.L. Research overview of high entropy alloy. *Trans. Mater. Health Treat.* **2020**, *41*, 37–48.
89. Gao, W.; Dong, Y.Q.; Jia, X.J.; Yang, L.P.; Li, X.B.; Wu, S.D.; Zhao, R.L.; Wu, H.; Li, Q.; He, A.N.; et al. Novel CoFeAlMn high-entropy alloys with excellent soft magnetic properties and high thermal stability. *J. Mater. Sci. Technol.* **2023**, *153*, 22–31. [[CrossRef](#)]

90. Feng, X.M.; Zheng, R.Y.; Wu, Z.Y.; Zhang, Y.; Li, Z.; Tan, X.H.; Xu, H. Study on a new high-entropy alloy $\text{Nd}_{20}\text{Pr}_{20}\text{La}_{20}\text{Fe}_{20}\text{Co}_{10}\text{Al}_{10}$ with hard magnetic properties. *J. Alloys Compd.* **2021**, *882*, 160640. [[CrossRef](#)]
91. Duan, J.C.; Wang, M.L.; Huang, R.; Miao, J.W.; Lu, Y.P.; Wang, T.G.; Li, T.G. A novel high-entropy alloy with an exceptional combination of soft magnetic properties and corrosion resistance. *Sci. China Mater.* **2023**, *66*, 772–779. [[CrossRef](#)]
92. Wang, T.; Wang, Y.G.; Wang, N.; Xu, S.; Han, Z.H.; Wang, Y. Development of a novel $(\text{Ni}_{40}\text{Fe}_{30}\text{Co}_{20}\text{Al}_{10})_{90}\text{Ti}_{10}$ high-entropy alloy with excellent photocatalytic performance. *Mater. Lett.* **2021**, *283*, 128817. [[CrossRef](#)]
93. Wu, F.Y.; Dou, Y.B.; Zhou, J.C.; Qin, J.B.; Jiang, T.; Yao, Y.C.; Zhang, W.J. High-entropy $(\text{FeCoNiCuZn})\text{WO}_4$ photocatalysts-based fibrous membrane for efficient capturing and upcycling of plastic. *Chem. Eng. J.* **2023**, *470*, 144134. [[CrossRef](#)]
94. Wail, A.Z.; Bassem, A.; Abdul, W.A.; Stefano, L.; Kang, J.H.; Young, G.K. Experimental and theoretical investigation of high-entropy alloy/support as a catalyst for reduction reactions. *J. Energy Chem.* **2023**, *81*, 132–142.

Disclaimer/Publisher's Note: The statements, opinions and data contained in all publications are solely those of the individual author(s) and contributor(s) and not of MDPI and/or the editor(s). MDPI and/or the editor(s) disclaim responsibility for any injury to people or property resulting from any ideas, methods, instructions or products referred to in the content.